proved to be very useful. The discrepancy in $\sigma_{v+rv}(\vartheta)$ between theory and experiment in the earlier investigations is found to be mainly due to $\sigma_v(\Delta j=0)$, while $\sigma_{rv}(\vartheta)$ agrees quite well.

b) The energy range around 12 eV is characterized by the superposition of direct scattering and Feshbach-resonances. It has been discussed that in the case of H_2 Feshbach-resonances may be expected to have $^2\Sigma_g^+$-configuration in most cases. For the decay into the electronic ground state of H_2, which is of interest here, the dominating partial wave is the s-wave. This type of resonance is effective for vibrational excitation, but less important for rotational excitation. Obviously, this conclusion depends on the configuration of the resonant state and of the final state of the molecule.

c) The direct scattering process is present as a background process in the whole energy range. The direct scattering amplitude normally contains several partial waves, so that one finds direct rotational as well as direct vibrational excitation. Usually, the angular distributions vary with energy much more rapidly than in the case of the resonance scattering mechanism. The relative importance of the direct scattering amplitude is decreasing with increasing quantum number of the exit channel ($v=0$ for elastic scattering; $v=1, 2, 3, \ldots$ for vibrational excitation). The contributions to elastic scattering are relatively large, the cross sections for rotational and vibrational excitation due to direct scattering are very small. — These findings are expected to be valid also for other molecules.

Acknowledgements

We would like to thank Prof. Dr. H. EHRHARDT for encouragement and stimulating discussions. The e−He data of D. ANDRICK and A. BITSCH were of great use for the measurements of this work. The help of M. EYB in performing angular distribution measurements is also greatfully acknowledged.

Experimental Study of Low Energy e-O_2 Collision Processes

F. LINDER and H. SCHMIDT

Fachbereich Physik der Universität Trier-Kaiserslautern

(Z. Naturforsch. **26 a**, 1617—1625 [1971]; received 1 July 1971)

Elastic scattering, vibrational excitation to $v=1$, 2, 3, 4 of the electronic ground state, and electronic excitation to the states $a^1\Delta_g$ and $b^1\Sigma_g^+$ of O_2 have been measured in a crossed beam apparatus for collision energies from nearly 0 eV to 4 eV. Differential and integral cross sections have been determined and calibrated on an absolute scale. From 15 vibrational levels of O_2^-, which could be observed as resonances in the cross sections, the spectroscopic constants for the vibrational structure of O_2^- have been derived: $\omega_e = 135$ meV and $\omega_e x_e = 1$ meV. The cross sections for vibrational excitation have the order of 10^{-18} cm². eV for the larger resonance peaks. Detailed cross sections have been listed in Table 1. The half width of the resonance can be estimated to $\Gamma \approx 0.5$ meV, which corresponds to a lifetime tof 10^{-12} sec for the O_2^- states. The angular dependence of pure resonance scattering is rather flat and not in accordance with the simplest theoretical model. An analysis of the angular dependence and of the rotational structure of the resonance in a somewhat extended model have been performed. — No electronically excited O_2^- states could be detected in the energy range up to 3 eV.

Introduction

Low energy e − O_2 collision processes are of special interest in high atmosphere physics. In a more general context, the e − O_2 system represents an interesting example for the study of reaction mechanisms of electron-molecule scattering. It is well known that higher vibrational states of O_2^-, which is a stable negative ion in its lower vibrational levels, play an important role in electron scattering processes at very low energies. The formation and decay of these resonant states can be explained within the frame of the Born-Oppenheimer approximation. They are interpreted as very low-lying shape resonances [1a] in contrast to an earlier interpretation as nuclear-excited Feshbach resonances [1b]. Because of the low resonance energies and the high centrifugal barrier these resonances show characteristic differences compared with other resonance types which are discussed in the preceding paper [2].

Reprints request to Dr. F. LINDER, NOAA Environmental Research Laboratories, *Boulder, Colorado 80302*, USA.

[1a] A. HERZENBERG, J. Chem. Phys. **51**, 4942 [1969].

[1b] J. N. BARDSLEY and F. MANDL, Reports on Progress in Physics **31**, 471 [1968].

[2] F. LINDER and H. SCHMIDT, Z. Naturforsch. **26 a**, 0000 [1971]; preceding paper.

The state of knowledge concerning the O_2^- ion and its role in $e-O_2$ scattering has been described in a recent paper by BONESS and SCHULZ [3]. The main existing results are several determinations of the energy positions of the lower autoionizing levels of O_2^- by total and elastic scattering experiments [4–6], a rough estimation of the total vibrational excitation cross section and of the lifetime of the resonant state from electron swarm experiments [7, 8], and an investigation of the threshold behaviour of some vibrational excitation channels by the trapped electron method [6]. Using additional data from differential elastic $e-O_2$ scattering Boness and Schulz were able to determine spectroscopic constants of the O_2^--ion and to construct an O_2^- potential-energy curve. The electron affinity of O_2, which had been discussed for many years, has recently been determined by laser photodetachment [9]. The new value of EA = 0.43 eV is in agreement with the value [10] which had been used by Boness and Schulz.

The present paper deals with two main aspects of low energy electron-molecule scattering, the spectroscopy of temporary negative molecular ions and the investigation of the importance of these ions for electron-molecule collision processes. For these purposes, detailed measurements of the formation and decay of the O_2^- resonant state have been performed. It can be shown in the following that the inelastic decay channels, in this case vibrational excitation to $v = 1$, 2, 3, and 4 of the O_2-molecule, are more suitable for negative molecular ion spectroscopy. As many as 15 vibrational levels of the O_2^- ion have been detected, from which the spectroscopic constants of the O_2^- ground state can be derived. Determinations of branching ratios and half widths, measurements of angular distributions, and an analysis of the rotational structure of the resonances have been carried out. These informations are necessary for a more detailed understanding of the reaction mechanisms in $e-O_2$ collision processes.

In addition to elastic scattering and vibrational excitation of the ground state of O_2, excitation to the low-lying electronically excited states $a\,^1\Delta_g$ and $b\,^1\Sigma_g^+$ has also been investigated. No resonances have been found in these channels up to 3 eV. All measurements have been normalized to an absolute scale because of the practical interest of these data.

Experimental

The crossed beam apparatus and the experimental procedure are the same as in the preceding paper and will not be described here again. The energy resolution was not sufficient to resolve separate rotational transitions in the $e-O_2$ measurements. The experimental problems concerning the angular distributions of the scattered electrons and the transmission properties of of the electron optical systems are more critical than in the $e-H_2$ measurements because of the very low energies and the relatively large ratio of collision energies. In all cases differential e–He scattering in the same energy range [11] has been measured for comparison as a test of the apparatus. In order to avoid changes in contact potentials small admixtures of O_2 have been added to the He gas in these test measurements. For the normalization of the cross sections to absolute units the recent total scattering data of SALOP and NAKANO [12] have been used. For energies below 2 eV they have been extrapolated with the aid of the older data of BRÜCHE [13].

Results and Discussion

Figure 1 shows two typical energy loss spectra. At low energies (left side) vibrational excitation of O_2 is enhanced by resonance scattering via the vibrationally excited O_2^- states (see Fig. 2). For energies outside the resonance region (right side) the cross sections for the inelastic processes are much smaller. Besides direct vibrational excitation to $v = 1$ of the O_2 ground state the spectrum shows electronic excitation of the metastable states $a\,^1\Delta_g$ and $b\,^1\Sigma_g^+$.

Figure 2 presents measured excitation functions for $v = 1$, 2, 3, and 4 of the electronic ground state of O_2 with true intensity ratios. Two independent runs of the energy dependence of elastic scattering are also shown in the upper part of the figure. The energy positions of the resonances, which are due to

[3] M. J. W. BONESS and G. J. SCHULZ, Phys. Rev. **A 2**, 2182 [1970].
[4] M. J. W. BONESS and J. B. HASTED, Phys. Lett. **21**, 526 [1966].
[5] J. B. HASTED and A. M. AWAN, J. Phys. **B 2**, 367 [1969].
[6] D. SPENCE and G. J. SCHULZ, Phys. Rev. **A 2**, 1802 [1970].
[7] R. D. HAKE, JR. and A. V. PHELPS, Phys. Rev. **158**, 70 [1967].
[8] A. HERZENBERG, J. Chem. Phys. **51**, 4942 [1969].
[9] R. CELOTTA, R. BENNETT, J. HALL, J. LEVINE, and M. W. SIEGEL, 23. Gaseous Electronics Conf., Hartford (Conn.) 1970.
[10] J. L. PACK and A. V. PHELPS, J. Chem. Phys. **44**, 1870 [1966].
[11] D. ANDRICK and A. BITSCH, to be published.
[12] A. SALOP and H. H. NAKANO, Phys. Rev. **A 2**, 127 [1970].
[13] E. BRÜCHE, Ann. Physik **83**, 1065 [1927].

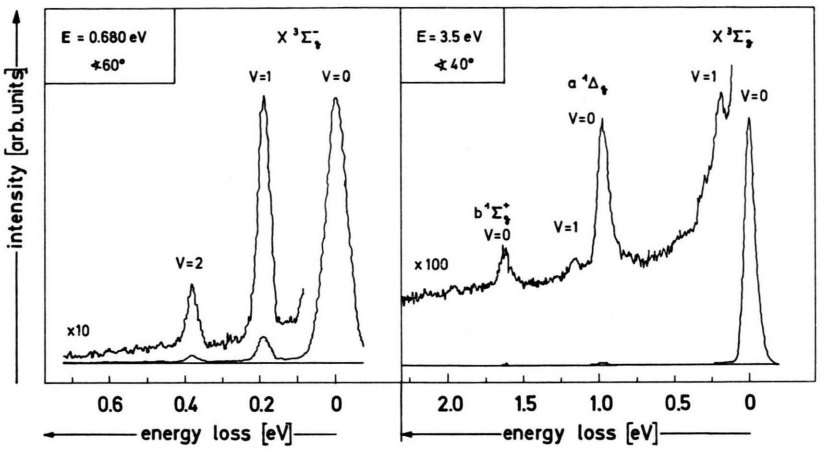

Fig. 1. Energy loss spectra for e—O_2 scattering. Collision energies, scattering angles, and the identification of the excited levels, are indicated. Left side: Resonant vibrational excitation at $E=0.680$ eV. Right side: Direct excitation of several levels at $E=3.5$ eV. The inelastic cross sections are much lower in this case.

the higher vibrational levels of the O_2^- $^2\Pi_g$-ground state, are indicated by vertical lines. They are determined from the inelastic channels, while the maxima in the elastic channel seem to be displaced possibly because of interference between resonance and potential scattering amplitudes. Direct excitation contributions seem to be very small in the inelastic channels. Most of the difference between stored signal and zero line (horizontal lines to each curve in Fig. 2) outside the resonance region is due to unphysical background, which can be proved by measuring energy loss spectra. As can be seen from the energy loss spectra of Fig. 1, the direct excitation cross section is roughly of the order of 1% compared with the resonance excitation cross section.

The absolute energy scale has been calibrated from the threshold onsets of the excitation functions (indicated by arrows). The onsets are mainly caused by background electrons with energy $E\approx 0$. The operation of the acceptor system in the threshold region of the excitation functions has been tested by measuring the well-known threshold behaviour of the He 2^3S excitation function [14]. This method of energy calibration seems to be more reliable in this case, because the well-known resonances like the He 19.31 eV resonance usually used as energy marks are too far away in energy. The energy scales for the excitation functions $v=1$ to 4 have been determined independently. The energetic coincidence of the resonance peaks of different excitaiton func-

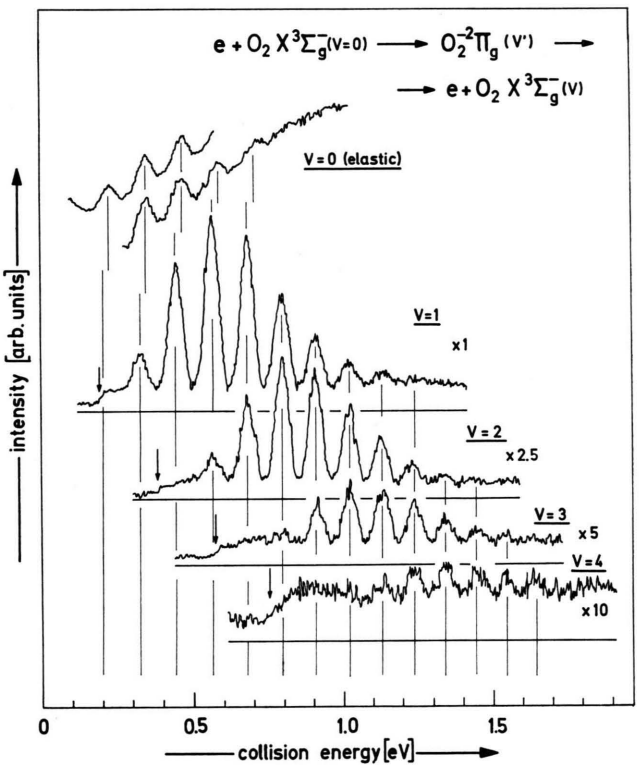

Fig. 2. Measured excitation functions for vibrational excitation to $v=1$, 2, 3, 4 of O_2 with true intensity ratios. The horizontal line at each curve indicates the zero line of the stored signal. Two runs of the energy dependence of elastic scattering are also shown in the upper part of the figure. The scattering angle is 60° for all curves. The vertical lines indicate the energy positions of the resonance peaks. The threshold onsets of the excitation functions are marked by small arrows. Energy-integrated cross sections in absolute units are listed in Table 1.

[14] H. EHRHARDT, L. LANGHANS, and F. LINDER, Z. Physik **214**, 179 [1968].

tions supports the reliability of the method. The error in the absolute energy scale is estimated to ± 20 meV. The determinations of relative energy positions have a much higher accuracy (about ± 1 meV within one curve).

Figure 3 compares measured angular distributions for (nearly) pure resonance scattering (peaks $v=1$ and $v=2$ of Fig. 1, left side) with model calcula-

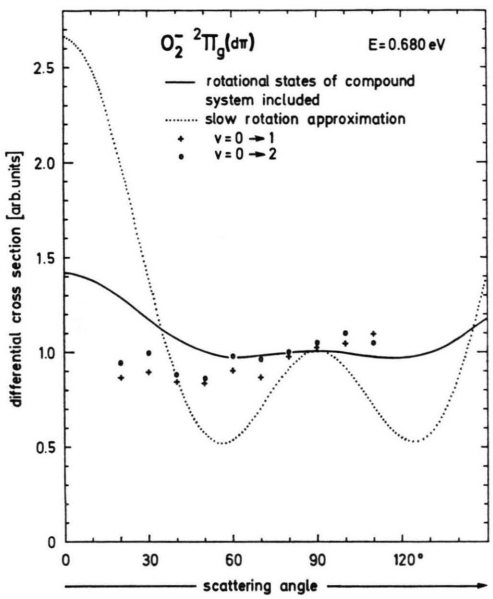

Fig. 3. Measured angular distributions for pure resonance scattering (peaks $v=1$ and $v=2$ of Fig. 1, left side) compared with two different model calculations which are discussed in the text. The curves have been normalized at or near 90°. The experimental error of the measured points is estimated to 10%.

tions based on the resonance scattering formalism of O'MALLEY and TAYLOR [15]. All results are arbitrarily normalized at or near 90°. The dotted curve represents the well-known slow rotation approximation with assumed $^2\Pi_g$-configuration of the resonant state and $d\pi$-approximation for the π_g-electron. This aproximation is applicable for those resonances where the lifetime of the resonance is short compared to the rotational period [16]. Since it is known from experimental and theoretical estimates [7, 8] and is also confirmed by our own experimental results described below that for these O_2^- resonant states a much longer lifetime has to be considered, one cannot expect that the slow rotation approximation is in agreement with experiment. We have therefore tried to extend the formalism of O'Malley and Taylor by including the rotational states of the compound system and simultaneously retaining all other approximations usually made. The result is shown as full line in Figure 3. A more explicit description of the derivation of this curve is given in Appendix A. The general structure is the same as in the slow rotation approximation, but the inclusion of a rotating compound system obviously flattens the angular distribution. A first consequence for experiment is that a much higher accuracy is necessary when this method shall be used for the classification of resonant states. Although an error of $\pm 10\%$ for each point must be considered, the experimental results seem to be well outside the calculated curve and would even be more for other choices of normalization. Since there is no doubt in this case that the O_2^- ion has $^2\Pi_g$-configuration, there must be

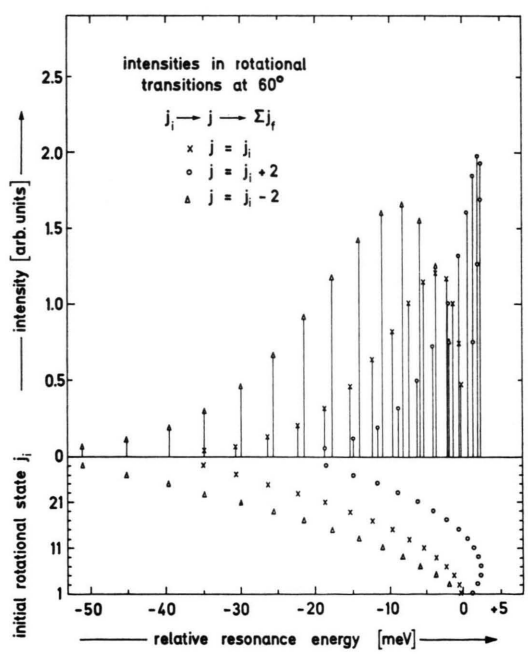

Fig. 4. Analysis of the rotational structure of the resonance peaks of Fig. 2. The upper part of the figure shows relative intensities in rotational transitions $j_i \rightarrow j \rightarrow \sum j_f$ for a scattering angle of 60°, the lower part indicates the corresponding energy positions in relative resonance energies as a function of the initial state j_i. The reference point of the energy scale belongs to the transition $j_i=0 \rightarrow j=0$, which is not actually present. There are three branches because of the selection rule $\Delta j=0, \pm 2$. The gas temperature was $T=67$ °C.

[15] T. F. O'MALLEY and H. S. TAYLOR, Phys Rev. **176**, 207 [1968]; see also: F. H. READ, J. Phys. B (Proc. Phys. Soc., Ser. 2) **1**, 893 [1968].

[16] H. EHRHARDT, L. LANGHANS, F. LINDER, and H. S. TAYLOR, Phys. Rev. **173**, 222 [1968].

another reason for the disagreement. Our model calculation, which has been performed in order to investigate the influence of a rotating compound system and which gives a reasonable result at a first glance, contains too many simplifications. Further theoretical investigation is needed in order to explain the measured angular distribution.

Figure 4 shows an analysis of the rotational structure of the resonance peaks, which is not resolved in the measurements of Figure 2. For a temperature of $T = 67\,^{\circ}\mathrm{C}$, at which the measurements have been performed, rotational states up to about $j_i = 35$ are populated with a maximum at $j_i = 9$. Only odd j_i are possible in the case of O_2. The lower part of Fig. 4 shows the energy positions of the resonances as a function of the initial rotational state j_i. Each resonance occurs at an electron energy which is the difference between the energies of resonant state and initial state. The energies have been calculated from the same formula as in the preceding paper [2, 17]. For O_2^- the internuclear distance $R_e(O_2^-) = 1.377$ A of BONESS and SCHULZ [3] has been used to determine the rotational constant B. The reference mark in the relative energy scale belongs to the (not actually present) transition $j_i = 0$ to $j = 0$. There are three branches because of the selection rule $\Delta j = 0, \pm 2$ for the formation of the resonant states. — The upper part of Fig. 4 shows the relative intensities for rotational transitions from a certain initial state j_i to a certain resonant state j, multiplied by the population of the initial state (see Appendix A). Each resonance line has a Breit-Wigner form of half width Γ, if the half width is assumed to be the same for all lines. Interference effects between overlapping resonances are neglected. Since the angular dependence is different for each resonance line, the rotational structure changes with angle. It is given for an angle of 60° in Fig. 4, because this structure is used for further analysis of the data of Fig. 1 (left side) and Fig. 2 which have been taken at 60°.

The analysis of the rotational structure depends to some extent on the model which has been used in the calculations. However, some general features should be independent of the model. The relative line intensities within one branch are mainly determined by the population numbers, while the relative intensities from one branch to the other should depend on the model. As general structure one gets a long tail to lower energies and a sudden decrease on the high energy side. It might be possible that the slowly rising direct excitation background found by SPENCE and SCHULZ [6] in trapped-electron experiments can be explained by this rotational tail of the resonances. This would be in agreement with our experiments which gave very low direct excitation in the whole energy range.

Table 1 summarizes the energy positions and the branching ratios for formation and decay of the resonant states. The assignment $v' = 4 \ldots 18$ for the resonant states assumes the electron affinity $EA = (0.43 \pm 0.03)$ eV recently determined by laser photodetachment [4]. From the energy differences, which can be determined with an accuracy of about 1 meV, the spectroscopic constants for the vibrational structure of O_2^- can be derived. From 14 independent values we get $\omega_e = 135$ meV and $\omega_e x_e = 1$ meV. BONESS and SCHULZ [3] found the same value for ω_e, but 1.5 meV for the anharmonicity.

The accuracy of the absolute energy calibration is estimated to ± 20 meV as discussed above. The energies given in Table 1 have been corrected by

Table 1.

		Resonance energies [in eV] and energy-integrated cross sections [in 10^{-20} cm^2 · eV]														
vibr. state v'		4	5	6	7	8	9	10	11	12	13	14	15	16	17	18
energy E[eV]		0.082	0.207	0.330	0.450	0.569	0.686	0.801	0.914	1.025	1.135	1.242	1.346	1.449	1.550	1.649
ΔE[meV]			125	123	120	119	117	115	113	111	110	107	104	103	101	99
	$v = 1$	×	—	25	82	110	100	61	35	17	9	5	—	—	—	—
exit	$v = 2$	×	×	×	—	8.5	25	32	28	19	12	5.8	2.4	1.1	—	—
channel	$v = 3$	×	×	×	×	—	—	1.3	5.5	7.3	7.0	5.8	3.3	1.8	1.0	—
	$v = 4$	×	×	×	×	×	×	—	—	—	1.0	1.9	2.0	1.7	1.3	1.0

[17] G. HERZBERG, Spectra of Diatomic Molecules, 2. Edition, van Nostrand Company, Princeton (N.J.) 1950.

6 meV compared to the energy positions of the peak maxima of Fig. 2 because of the rotational structure of the resonance. When the structure of Fig. 4 is folded with the product of the energy profiles of the gun and the acceptor, which corresponds to the experimental situation of Fig. 2, the peak maximum is found 6 meV below the $j_i = 0 \rightarrow j = 0$ transition. The corrected resonance energies listed in Table 1 correspond to the vibrational states of O_2^- with $j = 0$. It is remarkable that our energy calibration shows excellent agreement with the finding that the levels $v' = 8$ of O_2^- and $v = 3$ of O_2 (570 meV) coincide in energy, which was an important result in the measurements of SPENCE and SCHULZ [6]. Extrapolation of the vibrational levels to $v' = 0$ gives $EA = (0.44 \pm 0.02)$ eV in agreement with the laser photodetachment experiment [9].

For the determination of the energy-integrated cross sections in absolute units we have used the energy loss spectrum of Fig. 1 (left side). The first inelastic peak corresponds to excitation of $v = 1$ of O_2 via $v' = 9$ of O_2^-. The magnitude of the elastic cross section can be taken from Fig. 6. The ratio of the two peaks represents the ratio of the cross sections averaged over an energy distribution which is given by the product of the energy profiles of the gun and the acceptor. As described in more detail in Appendix B, this ratio yields an energy-integrated cross section of $8 \cdot 10^{-20}$ cm^2·eV/ster for $v = 1$, which corresponds to the area under the resonance profile of Figure 4. Since the angular dependence is nearly isotropic, the integration over all angles can be carried out by multiplying with 4π. This gives an energy- and angle-integrated cross section of $1 \cdot 10^{-18}$ cm^2·eV for the process

$$v_i = 0 \rightarrow v' = 9 \rightarrow v_f = 1 ,$$

summed and averaged, respectively, over all contributing rotational states. The error of this absolute determination is estimated to about 10% without the additional error inherent in the total cross section data. The energy-integrated cross sections of all resonance peaks of Fig. 2 have been listed in Table 1 in units of 10^{-20} cm^2·eV. The relative magnitudes can be falsified by transmission effects of the electron optical systems. However, since these transmission properties have been tested rather extensively, the errors should not be very large, i. e. not more than 20% for the ratio of a peak at the beginning to a peak near the end of one curve of Figure 2. It seems difficult to compare our results with the branching ratios of SPENCE and SCHULZ [6] because the trapped-electron method yields only the resonance peaks near threshold, which are small in size and not very well developed in our measurements. The absolute values, however, seem to be generally lower than ours, whereas the cross sections estimated from swarm experiments [7] have the same order of magnitude as the results of this work.

Only a rough estimation can be given for the half-width of the resonance lines of Fig. 4, because the branching ratios for the important exit channel $v = 0$ (elastic scattering) are not known from this experiment. Using the Breit-Wigner formula, the energy-integrated cross section is equal [8, 18] to

$$2\pi^2 \lambda\!\!\!^{-2}\, g \frac{\Gamma_i \Gamma_f}{\Gamma} .$$

$2\pi\,\lambda\!\!\!^{-}$ is the de Broglie wave length of the incoming electron at $E = 0.680$ eV, g is a spin weight factor, Γ_i is the partial width for formation of the resonant state $v' = 9$ from the initial state $v_i = 0$, Γ_f is the partial width for the decay of this resonant state to the final state $v_f = 1$, and $\Gamma = \Sigma \Gamma_f$ is the total width. Γ_i also determines the decay of the resonant state into the elastic channel. Since the branching ratios decrease with the quantum number of the exit channel, we assume $\Gamma_i \approx 2\,\Gamma_f$ in a very rough estimate and hence $\Gamma \approx 3\,\Gamma_f \approx 1.5\,\Gamma_i$. It follows that Γ is of the order of 0.5 meV, which gives a life-time of 10^{-12} sec for the resonance. This estimation confirms that a rotating compound system has to be considered in the calculations of the angular dependence, since the rotational period of O_2^- has also the order of 10^{-12} sec for $j = 9$.

In the course of this work the exit channels $v = 0$ to $v = 4$ of the electronic ground state and additionally the low-lying electronic states $a\,^1\Delta_g$ and $b\,^1\Sigma_g^+$ have been examined for further i. e. electronically excited O_2^- states. This question is of interest in connection with the variety of determinations of the electron affinity [19] of O_2. No other O_2^- states besides the vibrationally excited $^2\Pi_g$ resonances could be found in the energy range up to 3 eV. The $a\,^1\Delta_g$

[18] J. M. BLATT and V. F. WEISSKOPF, Theoretical Nuclear Physics, John Wiley & Sons, New York 1952.

[19] See Ref. [3] for a list of references.

and $b\,^1\Sigma_g^+$ channels seem to be free of resonances in this energy range in spite of the fact that they are energetically accessible for the higher vibrational levels of the O_2^- state. The cross sections for excitation of these states up to 4 eV have been determined in absolute units because of their practical interest in high atmosphere physics. They are shown in Fig. 5 together with the results of a semiempirical theory [20]. The experimental results are in excellent agreement with recent results of TRAJMAR et al. [21] who determined the excitation of these states from 4 eV up to higher collision energies. Our results complete the information on these processes to lower energies.

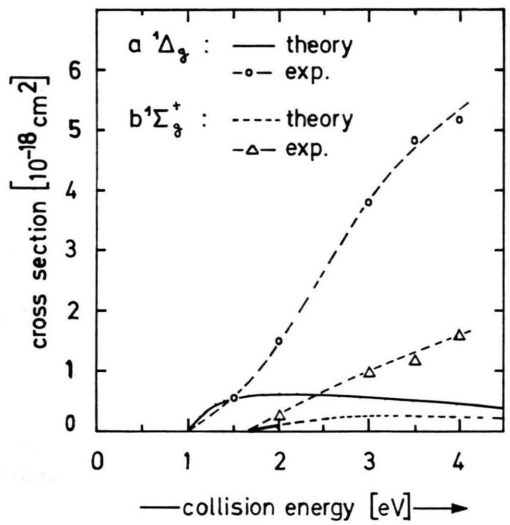

Fig. 5. Integral cross sections in absolute units for excitation of the states $a\,^1\Delta_g$ ($v=0$) and $b\,^1\Sigma_g^+$ ($v=0$) of O_2. The measured cross sections are compared with the results of a semiempirical theory [20]. The experimental errors are in the order of 20%.

Finally, Fig. 6 shows angular distributions of elastic scattering outside the resonances. The experimental procedure is the same as described elsewhere [2]. For normalization to absolute units the total cross section data of SALOP and NAKANO [12] have been used, which had to be extrapolated from 2 eV to lower energies. Without the error of these data, we estimate an error of 5 – 10% for each point. It seems remarkable that the angular distributions show a decrease at small angles even for energies up to 4 eV. This is unusual compared to other molecules. Pronounced forward scattering does not show up until the energy exceeds 10 eV as can be seen from the measurements of TRAJMAR et al. [21].

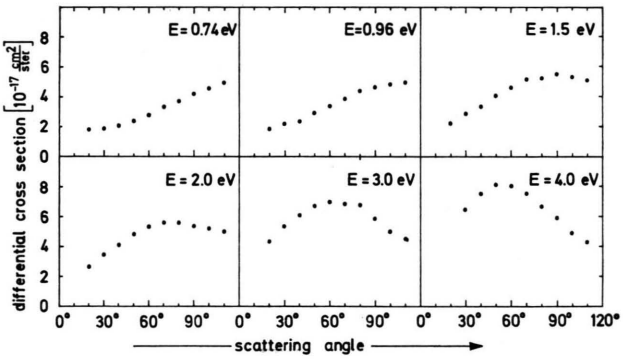

Fig. 6. Measured angular distributions for non-resonant elastic scattering from O_2. The differential cross sections are presented in absolute units. The collision energies are indicated in the figure.

Conclusions

Detailed experimental investigations of low energy e – O_2 collision processes have yielded a lot of information on the role of O_2^- resonant states in these collisions. The results demonstrate the use of high-resolution electron spectroscopy for negative molecular ion spectroscopy. The determination of differential and integral cross sections in absolute units for all collision processes is of practical interest especially in the low energy region. The e – O_2 system represents an interesting example for the study of reaction mechanisms in electron-molecule collisions. The resonant states are interpreted as shape resonances, but the very large centrifugal barrier compared to the very low resonance energies gives rise to a much longer lifetime than in the case of other well-known shape resonances. A model calculation has been performed in which the rotational states of the compound system have been included. However, the discussion shows that probably too many simplifications are inherent and that the experimental results need further theoretical analysis.

[20] C. E. WATSON, V. A. DULOCK, JR., R. S. STOLARSKI, and A. E. S. GREEN, J. Geophys. Res. **72**, 3961 [1967].

[21] S. TRAJMAR, D. C. CARTWRIGHT, and W. WILLIAMS, to be published.

Appendix A

The matrix element for pure resonance scattering can be written [15]

$$T_{\mathrm{fi}} = \sum_{\Lambda v j m} \frac{\langle \Psi^{(\mathrm{f})}_{v_{\mathrm{f}} j_{\mathrm{f}} m_{\mathrm{f}}} | V | \Psi^{(\mathrm{r})}_{vjm} \rangle \langle \Psi^{(\mathrm{r})}_{ojm} | V | \Psi^{(\mathrm{i})}_{o_{\mathrm{i}} j_{\mathrm{i}} m_{\mathrm{i}}} \rangle}{E - (E_{\mathrm{r}} + E_{\mathrm{v}} + E_{\mathrm{j}}) + i\,\Gamma/2} \tag{A 1}$$

where i, r, and f denote initial, resonant, and final state. The dominator contains the energies $E_{\mathrm{r}} + E_v + E_j$ of the resonant states and the half width Γ, which for simplicity is assumed to be independent of v and j. It is summed over all resonant states with quantum numbers v, j, and m, while the sum over Λ runs only over the two values $\pm|\Lambda_{\mathrm{r}}|$ of the resonant state. The zero order wave functions are in adiabatic approximation

$$\Psi(\boldsymbol{r}, \boldsymbol{R}) = \Phi_{\mathrm{el}}(\boldsymbol{r}, \boldsymbol{R}) \cdot \zeta_{\mathrm{n}}(\boldsymbol{R}) = \Phi_{\mathrm{el}}(\boldsymbol{r}, \boldsymbol{R}) \cdot \chi_{\mathrm{v}}(R) \cdot \frac{1}{R} \cdot Y_{\mathrm{jm}}(\hat{R}) \tag{A 2}$$

where it must be noted that for the initial and the final state the electronic part of the wave function depends not only on the internuclear distance R, but also on the orientation of the molecule.

The procedure in the model calculation of Fig. 3 is now as follows. The differential cross section $\sigma(v_{\mathrm{i}} \rightarrow v_{\mathrm{f}})$ for purely resonant vibrational excitation is proportional to

$$\sum_{j_{\mathrm{i}}} P_{j_{\mathrm{i}}} \sum_{j_{\mathrm{f}}} \frac{1}{2\,j_{\mathrm{i}} + 1} \sum_{m_{\mathrm{i}}} \sum_{m_{\mathrm{f}}} |T_{\mathrm{fi}}|^2 . \tag{A 3}$$

In the usual way, it has been summed over final substates m_{f} and averaged over initial substates m_{i}. The sum over j_{f} takes into acount that the final rotational states j_{f} are not separated in the experiment. The remaining sum averages over all contributing initial rotational states j_{i}. The numbers $P_{j_{\mathrm{i}}}$ give the population of the rotational states for a temperature of $T = 67\,^{\circ}\mathrm{C}$, at which the measurements have been performed. Only rotational states with odd j_{i} are occupied. The sum includes rotational states up to $j_{\mathrm{i}} = 35$.

Now following the procedure of O'MALLEY and TAYLOR [15] (except using the slow rotation approximation) and approximatinig the π_g-electron by a $d\pi$-electron one gets the following form for the matrix element for vibrational excitation $v_{\mathrm{i}} \rightarrow v_{\mathrm{f}}$ via a certain resonant state v (the vibrational states v of the resonance are well separated in the experiment, see Fig. 2):

$$T_{\mathrm{fi}} = F(v_{\mathrm{i}}, v_{\mathrm{f}}, v) \sum_{j, m, \Lambda = \pm 1} \frac{\langle Y_{j_{\mathrm{f}} m_{\mathrm{f}}}(\hat{R}')\; Y_{2\Lambda}(\hat{k}_{\mathrm{f}}) \,|\, Y_{jm}(\hat{R}') \rangle \langle Y_{jm}(\hat{R}) | Y_{2\Lambda}(\hat{k}_{\mathrm{i}})\; Y_{j_{\mathrm{i}} m_{\mathrm{i}}}(\hat{R}) \rangle}{E - (E_{\mathrm{r}} + E_{\mathrm{v}} + E_{\mathrm{j}}) + i\,\Gamma/2} . \tag{A 4}$$

$F(v_{\mathrm{i}}, v_{\mathrm{f}}, v)$ is a vibrational factor which is not of interest here. This matrix element, in which the rotational states of the compound system are included, is inserted in (A 3). It has been assumed in the calculations that the width of the resonance peaks is small compared to their separation from each other (see Fig. 4), so that the sum over j can be carried out incoherently. The result for Γ (see text) shows that this assumption is not too bad for many lines. The result of the calculation is the full line in Fig. 3, while the dotted line is the well-known slow rotation approximation.

From the same calculation, but before summing over j and j_{i}, one gets relative intensities for rotational transitions from a certain initial state j_{i} to a certain resonant state j, multiplied by the population $P_{j_{\mathrm{i}}}$ of the initial state. Because of the selection rule $\Delta j = 0, \pm 2$ there are three possible resonant states for each j_{i}. The decay of each resonant state into all final states (again three of them) has already been included in the relative intensities by the summation over j_{f}. The results are the line intensities shown in Figure 4.

Appendix B

We want to analyze the energy loss spectrum in Fig. 1, left side. The signal detected at the multiplier for a fixed scattering angle is proportional to

$$S' = \int \sigma(E)\, f_{\mathrm{g}}(E - E_{\mathrm{g}})\, f_{\mathrm{a}}(E - E_{\mathrm{a}})\, \mathrm{d}E . \tag{B 1}$$

$f_{\mathrm{g}}(E - E_{\mathrm{g}})$ and $f_{\mathrm{a}}(E - E_{\mathrm{a}})$ are the energy profiles of the gun and the acceptor with mean energies E_{g} and E_{a}, respectively. In the case of vibrational ex-

citation, the cross section $\sigma_v(E)$ is represented by the line spectrum of Fig. 4 of this paper, which has a centre of intensity at $E_0 = -6$ meV in relative resonance energies as already mentioned in the text. One gets the maximum of inelastically scattered electrons for $E_g = E_0$ and the maximum of detected current, if also $E_a = E_0 - W$, where W is the energy loss of the scattered electrons. The elastic cross section $\sigma_{el}(E)$ can be assumed as nearly constant over the energy range of the functions f_g and f_a. Under these conditions and with the absolute elastic cross section of Fig. 6, one gets from the ratio of the peak maxima in Fig. 1: $S'_{v=1} = 6.7 \cdot 10^{-20}$ cm^2 eV/ster. We have assumed Gaussian profiles for f_g and f_a, the half widths of which were $\Delta E_g = 58$ meV and $\Delta E_a = 31$ meV, respectively, in accordance with the data of the selectors (slit width, mean radius, transmision energy). The measured half widths of the elastic peak ($\Delta E = 65$ meV) and the inelastic peak ($\Delta E = 35$ meV) in Fig. 1 are consistent with all assumptions of this appendix.

In $S'_{v=1}$, the outer lines of the structure of Fig. 4 are suppressed by the energy profiles f_g and f_a. A correction of 20% must be applied to get the energy-integrated cross section

$$S_{v=1} = \int \sigma_{v=1}(E)\, dE\,, \qquad \text{(B 2)}$$

which is the desired final result. This gives $S_{v=1} = 8 \cdot 10^{-20}$ cm^2 eV/ster which corresponds to the area under the resonance structure of Figure 4.

Interaction of Randomly Phased Vibrational Waves via the Collision Dominated Solid State Plasma

W. WONNEBERGER

Physikalisches Institut der Universität Freiburg i. Br.

(Z. Naturforsch. **26 a**, 1625—1629 [1971]; received 24 July 1971)

A diagrammatic technic is presented which is appropriate to study the nonlinear response of the collision dominated solid state plasma to randomly phased ac fields. By summation of diagrams, a nonlinear integral equation is established for the propagator S' which is directly related to the nonlinear response function. Using the equation for S', an equivalence is derived between a model solution in the theory of nonlinear coherent ultrasound amplification and the interaction theory of a great number of randomly phased vibrational modes, confined to a small frequency band.

1. Introduction

It has been proposed by HUTSON [1] that the interaction of highly amplified vibrational waves in a piezoelectric semiconductor predominantly proceeds via the electron gas by means of the concentration nonlinearity. An ultrasonic wave produces an accompanying electric field which perturbs the electron gas. The electron gas usually is in the state of a collision dominated plasma. In this case, the Coulomb interaction of the electrons manifests itself in form of the concentration nonlinearity. The theory of vibrational wave interactions in a piezoelectric semiconductor thus essentially is equivalent to the study of the nonlinear response of the collision dominated solid state plasma.

In recent years, the following special case has attracted some attention: The great number of acoustoelectrically active modes present in the crystal may be treated in the random phase approximation (RPA). More precisely, one assumes that these waves are subject to a Gaussian random process. One of the first investigators to treat this problem, were YAMADA [2] and GUREVICH et al. [3] who derived on this basis transport equations for the phonon distribution function. Recently, RIDLEY and WILKINSON [4], GANGULY and CONWELL [5], and BUTCHER and SLECHTA [6] investigated the acoustoelectric gain of vibrational waves within the RPA.

All these authors confine themselves to the lowest orders in perturbation theory.

[1] A. R. HUTSON, Phys. Rev. Lett. **9**, 296 [1962].
[2] K. YAMADA, Phys. Rev. **169**, 690 [1968].
[3] V. L. GUREVICH, V. D. KAGAN, and B. D. LAIKHTMAN, Sov. Phys. JETP **27**, 102 [1968].
[4] B. K. RIDLEY and J. WILKINSON, Brit. J. Phys. C **2**, 1307 [1969].
[5] A. K. GANGULY and E. M. CONWELL, Phys. Lett. **29 A**, 271 [1969].
[6] P. N. BUTCHER and J. SLECHTA, Brit. J. Phys. C **4**, 870 [1971].